

## Graded-size Si quantum dot ensembles for efficient light-emitting diodes

A. Anopchenko, A. Marconi, M. Wang, G. Pucker, P. Bellutti, and L. Pavesi

Citation: [Applied Physics Letters](#) **99**, 181108 (2011); doi: 10.1063/1.3658625

View online: <http://dx.doi.org/10.1063/1.3658625>

View Table of Contents: <http://scitation.aip.org/content/aip/journal/apl/99/18?ver=pdfcov>

Published by the [AIP Publishing](#)

---

### Articles you may be interested in

[Nanocrystalline-Si-dot multi-layers fabrication by chemical vapor deposition with H-plasma surface treatment and evaluation of structure and quantum confinement effects](#)

[AIP Advances](#) **4**, 017133 (2014); 10.1063/1.4864055

[Graded-size Si-nanocrystal-multilayer solar cells](#)

[J. Appl. Phys.](#) **112**, 104304 (2012); 10.1063/1.4766307

[Structure of Si-capped Ge/SiC/Si \(001\) epitaxial nanodots: Implications for quantum dot patterning](#)

[Appl. Phys. Lett.](#) **100**, 141603 (2012); 10.1063/1.3699223

[A Si-based quantum-dot light-emitting diode](#)

[Appl. Phys. Lett.](#) **86**, 103509 (2005); 10.1063/1.1882757

[Band gap engineering of amorphous silicon quantum dots for light-emitting diodes](#)

[Appl. Phys. Lett.](#) **78**, 2575 (2001); 10.1063/1.1367277

---

The advertisement features a dark blue background with white and orange text. At the top left, it reads 'NEW! Asylum Research MFP-3D Infinity™ AFM' in large white letters, followed by 'Unmatched Performance, Versatility and Support' in orange. On the right, the Oxford Instruments logo is shown with the tagline 'The Business of Science®'. Below the text are several images: a blue textured surface, a brown textured surface, a grid of small square samples, and the MFP-3D Infinity AFM instrument itself. Text boxes describe the instrument's capabilities: 'Stunning high performance', 'Simpler than ever to GetStarted™', 'Comprehensive tools for nanomechanics', and 'Widest range of accessories for materials science and bioscience'.

## Graded-size Si quantum dot ensembles for efficient light-emitting diodes

A. Anopchenko,<sup>1,a)</sup> A. Marconi,<sup>1</sup> M. Wang,<sup>1,2,b)</sup> G. Pucker,<sup>2</sup> P. Bellutti,<sup>3</sup> and L. Pavesi<sup>1</sup>

<sup>1</sup>*Nanoscience Laboratory, Department of Physics, University of Trento, Via Sommarive 14, Povo 38123, Italy*

<sup>2</sup>*Advanced Photonics and Photovoltaics, FBK, Via Sommarive 18, Povo 38123, Italy*

<sup>3</sup>*MicroTechnologies Laboratory, FBK, Via Sommarive 18, Povo 38123, Italy*

(Received 21 June 2011; accepted 17 October 2011; published online 1 November 2011)

We propose a simple way to engineer the energy band gap of an ensemble of silicon nanocrystal (Si-NC) embedded in SiO<sub>2</sub> via thickness/composition profiling of Si-NC multilayers. By means of a complementary metal-oxide-semiconductor compatible process, light emitting diodes (LEDs) which incorporate graded energy gap Si-NC multilayers in the active region have been grown. Electrical and optical properties of these graded Si-NC LEDs demonstrate the ability of the proposed method to tailor the optoelectronic properties of Si-NC devices. © 2011 American Institute of Physics. [doi:10.1063/1.3658625]

Engineering of energy band gap of semiconductor nanocrystals promises a high impact in photonic and biomedical applications, as demonstrated with colloidal nanocrystals of compound semiconductors.<sup>1–5</sup> Band gap engineering of silicon nanocrystals (Si-NCs) and their dense structurally ordered ensembles is studied to a much less extent (see, for example, Refs. 6 and 7) even though Si-NCs have a high potential impact in photonic applications.<sup>8</sup>

Here, we propose to engineer the energy band gap of dense Si-NC quantum dot ensembles via thickness/composition profiling of a multilayer (ML) Si-NC/SiO<sub>2</sub> structure. A ML approach allows the independent control of Si-NC size and density.<sup>9–11</sup> Upon annealing at a high-temperature, the thickness of non-stoichiometric silicon-rich silicon oxide (SRO) in the ML structure confines the nanocrystals size, while the excess silicon content of the SRO layer determines the nanocrystal density.<sup>11,12</sup> A control over the silicon oxide scaffolds is possible which ensures efficient injection and tunnelling currents in Si-NC light emitting diodes (LEDs). The Si-NC LEDs having a ML structure show high power efficiency and low operating voltages,<sup>13</sup> both provided by direct tunnelling of electrons and holes among the nanocrystals.<sup>14</sup> Indeed, we measured a power efficiency of the graded gap Si-NC LED of 0.20% which is comparable with the best Si-based LEDs reported so far.<sup>15</sup>

Since in ML LEDs the bipolar tunnelling of electrical charges at low voltages was achieved,<sup>14</sup> we propose a significant improvement of this scheme where the sizes of the nanocrystals increase from the active region towards the electrodes. In this way, the energy levels of the confined states in each layer gradually increase from the silicon value, so that reducing the energy difference between adjacent tunnelling states. Moreover, the luminescence efficiency increases due to the presence of small nanocrystals in the active region.<sup>15,16</sup>

The details on the fabrication of the ML Si-NC LED and of their properties can be found elsewhere.<sup>17,18</sup> The ML structure and formation of Si-NCs were confirmed by both

ellipsometry and high resolution transmission electron microscopy (TEM).<sup>17</sup> The actual thicknesses of the individual layers within the ML stack were somewhat smaller than the nominal thickness values. This is due to a delay in plasma ignition during the plasma-enhanced chemical vapor deposition (PECVD) growth and interdiffusion at the ML interfaces during the high temperature annealing. The total ML thickness is found to decrease of about 30% of its nominal value.<sup>17</sup>

Several Si-NC ML structures are studied: periodic MLs with a nominal ML period of 4 nm (2 nm SiO<sub>2</sub>/2 nm SRO), 5 nm (2 nm SiO<sub>2</sub>/3 nm SRO), and 6 nm (2 nm SiO<sub>2</sub>/4 nm SRO), having five ML periods each and a ML with graded SRO thickness. The graded ML has a stepwise decrease in the SRO thickness toward the ML centre (exact sequence of SRO layer thicknesses, in nanometers, is 4-3-2-2-3-4, see Fig. 1) and approximately the same average silicon content as the periodic ML of 3 nm SRO. All the SRO layers have the same composition. A schematic energy band diagram of a periodic and the graded-size (energy gap) Si-NC MLs is shown in Fig. 1. When *an external bias is applied*, the energy bands of the graded-size Si-NC ensemble align at low voltages (Fig. 1) which makes it easier for charges to tunnel into the central recombination region.

The formation of Si-NCs in ML structures is evidenced by the electroluminescence (EL) spectra shown in Fig. 2. The EL spectra of three MLs were collected at the same injection current density of 1 mA/cm<sup>2</sup>. The peak EL intensity of the graded Si-NC ML is about 3 times larger than the one of the reference periodic ML with 3-nm-thick SRO layer (approximately the same average excess silicon content). The peak wavelength blueshifts when the applied voltage increases which is shown in the inset of Fig. 2. This blueshift is ascribed to small variations in the nanocrystal size of a periodic ML structure.<sup>13</sup> In the whole range of applied voltages, the peak wavelength of the graded ML is smaller than the peak wavelength of the periodic ML with 3-nm-thick SRO, which is in turn smaller than the peak wavelength of the ML with 4-nm-thick SRO. This is in a good agreement with the quantum confinement effect. Together with the minor blueshift of the peak wavelength and large EL intensity, it also indicates that the light emission of the graded

<sup>a)</sup>Electronic mail: anopchenko@science.unitn.it.

<sup>b)</sup>Present address: Astronergy Solar, 1335 Binan Road, Hangzhou 310053, People's Republic of China.

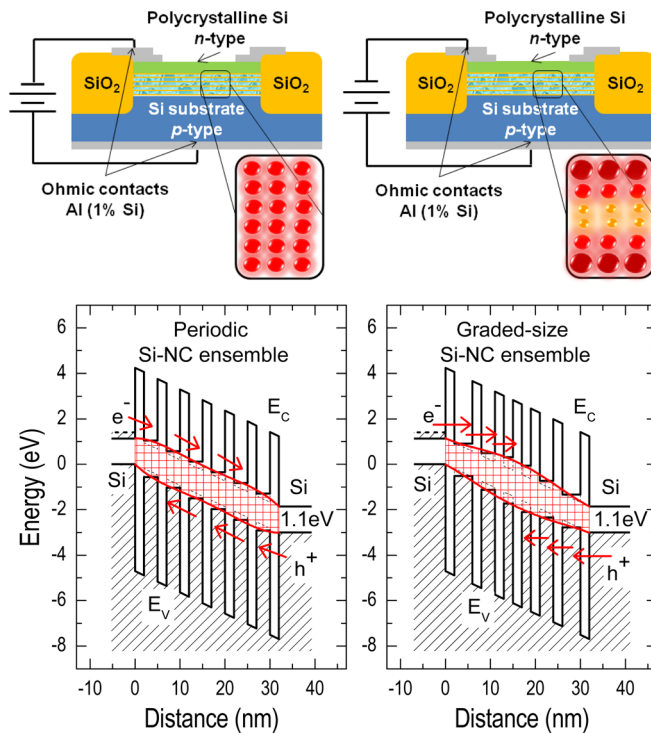


FIG. 1. (Color online) (Top) Schematic of the ML Si-NC LED with periodic (left) and graded size (right) Si-NC ensembles. (Bottom) Energy band diagram for a periodic (left) and the graded nanocrystal size ML Si-NC LED (right).  $E_C$  and  $E_V$  stand for the bottom of the conduction and the top of the valence energy bands, respectively. The checked pattern areas highlight the difference in the energy band gap of the active recombination region of the two LEDs. Notice an even alignment of the (electron and hole) ground states of Si-NC quantum dots and wider band gap in the middle of the active region of the graded-size LED. The arrows show direct tunneling (followed by a rapid thermalization) of electrons ( $e^-$ ) and holes ( $h^+$ ) from the cathode and anode, respectively.

ML originates mostly from the 2-nm-large nanocrystals in the centre of the ML stack.

Another evidence for the improved charge injection in the graded ML and light emission originating from the small-

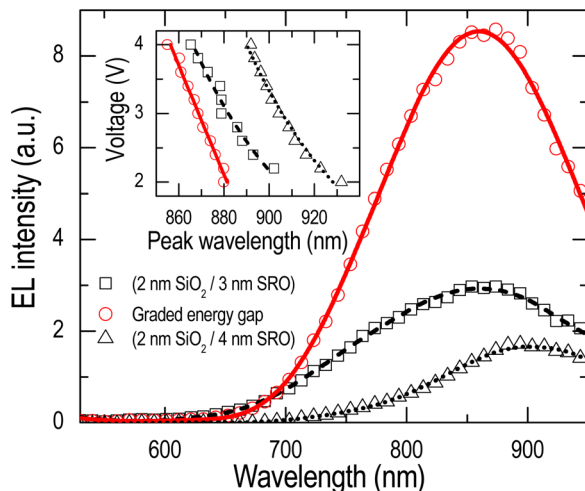


FIG. 2. (Color online) EL spectra of three Si-NC ML LEDs: periodic LED, 2 nm  $\text{SiO}_2$ /3 nm SRO; periodic LED, 2 nm  $\text{SiO}_2$ /4 nm SRO; and the LED with a graded energy gap. The spectra are taken at the same injection current density of 1  $\text{mA}/\text{cm}^2$ . The spectra are normalized to the spectrometer response. The inset shows the peak wavelength dependence on the applied voltage. Lines are a guide to the eye.

est nanocrystals could be found in Fig. 3. It shows current-voltage (I-V) characteristics of the three ML devices. The charge injection is enhanced in the graded ML with respect to the reference periodic ML with 3-nm-thick SRO. The ML with 4-nm-thick SRO is more conductive due to higher average silicon content,<sup>13,17</sup> larger Si-NCs and, hence, smaller band offset with respect to the silicon electrodes. On the contrary, the ML of 2 nm  $\text{SiO}_2$ /2 nm SRO shows poor electrical conduction, which becomes unstable when high voltages are forced, and no EL. This is attributed to the large band offset with respect to the silicon electrodes and to the low average silicon excess. The inset of Fig. 3 shows stretched exponential EL decay time as a function of the applied voltage (the stretching exponent of  $0.62 \pm 0.05$  is approximately constant within the voltage range and the same for all the devices). Again, the graded ML has the shortest decay time, which corresponds to the smallest excited nanocrystals. The EL decay time of the graded ML has almost a constant value of 60  $\mu\text{s}$  at low applied voltages when direct charge tunnelling is a dominant injection mechanism.<sup>14</sup> In contrast, the EL decay time of the periodic MLs decreases when applied voltage increases, which is ascribed to the excitation of smaller nanocrystals. The absence of the decay time voltage dependence indicates that the band offset tuning in the graded ML facilitates the carrier injection into the smallest nanocrystals. Our graded ML LED bears some resemblance with the best porous silicon LEDs which have graded porosity of the optically active and contact layers.<sup>15,16</sup>

The graded-size structure is a good compromise between an ensemble of large Si-NCs with high electrical conductivity, but low luminescence, and an ensemble of small Si-NCs with high luminescence, but poor electrical conductivity. Indeed, radiative recombination rate increases when nanocrystal size decreases<sup>9</sup> and, hence, an ensemble of small nanocrystals have larger emission efficiency than an ensemble of large nanocrystals. However, injection into small nanocrystals is hindered by a larger band offset of small Si-NC with respect to bulk silicon than that of large Si-NC. In contrast, an ensemble of large Si-NC (with lower

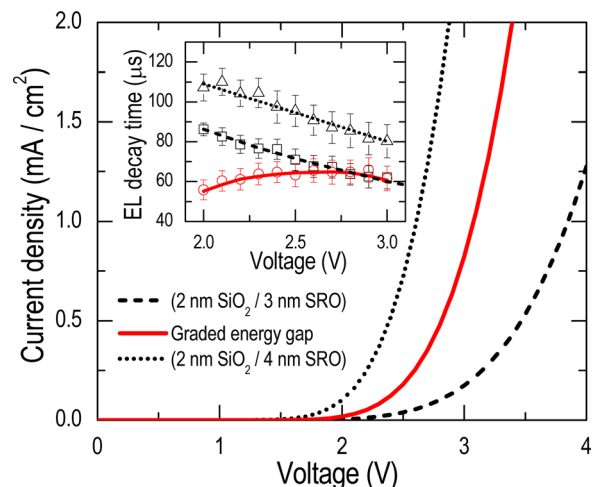


FIG. 3. (Color online) Forward I-V characteristics of the same three devices as in Fig. 2. The inset shows EL decay time for these devices as a function of the applied voltage (lines are a guide to the eye). EL signal was recorded under a pulse excitation scheme. The driving electrical signal has a frequency of 500 Hz.

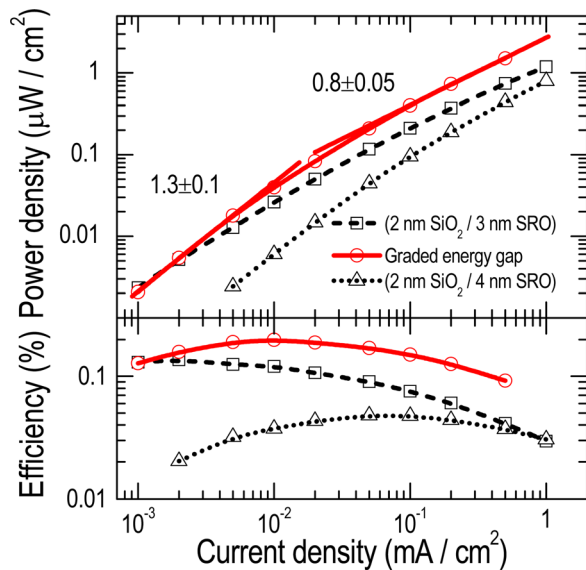


FIG. 4. (Color online) Optical power density as a function of injected electrical current density for the same three LEDs as in Fig. 2. Numbers indicate slope values of linear regressions. The bottom panel shows the corresponding power efficiency.

energy band offset) exhibits large conductivity, but low emission efficiency. The graded gap structure, with a step-like increase in band offset, provides a desired compromise between high recombination rates (in small Si-NC) and large injection currents (in an ensemble of large Si-NC). When external bias is applied, energy band alignment of the graded-size Si-NC ensemble is achieved over a range of low voltages (Fig. 1).

Optical power density of our devices, along with the corresponding power efficiency  $\eta$ , as a function of the injection current density,  $J$ , is shown in Fig. 4. The optical power dependence obeys a power law,  $\sim J^s$ . A super-linear increase with  $s = 1.3 \pm 0.1$  at low  $J$  and a sub-linear increase with  $s = 0.8 \pm 0.1$  at high  $J$  are observed. The super-linear dependence is attributed to the presence of radiative and non-radiative competing recombination channels. As  $J$  increases, the radiative recombination of excitons in Si-NCs takes over the recombination at non-radiative centres in the oxide matrix. At  $J \sim 10 \mu\text{A}/\text{cm}^2$ , recombination at the non-radiative centres saturates and optical power becomes an almost linear function of the current. At  $J \geq 10 \mu\text{A}/\text{cm}^2$ , non-radiative Auger recombination becomes dominant and EL becomes a sub-linear function of  $J$ .  $\eta$  of the graded-size LED reaches a maximum of 0.2% at  $J = 10 \mu\text{A}/\text{cm}^2$  and applied voltage of 2 V.  $\eta$  is about twice  $\eta$  of the corresponding periodic ML

LED at the same  $J$ . The maximum optical power density is as high as  $10 \mu\text{W}/\text{cm}^2$  (not shown here).

In conclusion, we show that (1) energy band gap engineering of Si-NC ensembles grown by PECVD or a similar complementary metal-oxide-semiconductor (CMOS) compatible technique is possible with the size-controlled ML approach and (2) the graded-size Si-NC LED shows superior performance in terms of power efficiency than periodic ML Si-NC LED. Therefore, this work shows that tunnelling engineering (control of the tunnelling barrier and injection energy) of electrical injection into Si-NCs might further improve the emission properties of the LED.

This work was supported by Intel Corporation and EC through the project ICT-FP7-224312 HELIOS. We acknowledge discussions with Zeno Gaburro. We thank Enrico Moser for the help with the time-resolved EL and Silvia Larcheri for the TEM images.

- <sup>1</sup>D. V. Talapin, J.-S. Lee, M. V. Kovalenko, and E. V. Shevchenko, *Chem. Rev.* **110**, 389 (2010).
- <sup>2</sup>Y. Yin and A. P. Alivisatos, *Nature* **437**, 664 (2005).
- <sup>3</sup>A. J. Nozik, M. C. Beard, J. M. Luther, M. Law, R. J. Ellingson, and J. C. Johnson, *Chem. Rev.* **110**, 6873 (2010).
- <sup>4</sup>S. Coe, W.-K. Woo, M. Bawendi, and V. Bulovic, *Nature* **420**, 800 (2002).
- <sup>5</sup>T. Franzl, T. A. Klar, S. Schietinger, A. L. Rogach, and J. Feldmann, *Nano Lett.* **4**, 1599 (2004).
- <sup>6</sup>I. Balberg, in *Silicon Nanocrystals: Fundamentals, Synthesis and Applications*, edited by L. Pavesi and R. Turan (Wiley, Berlin, 2010), p. 69.
- <sup>7</sup>V. A. Belyakov and V. A. Burdov, *J. Comput. Theor. Nanosci.* **8**, 1 (2011).
- <sup>8</sup>Z. Yuan, A. Anopchenko, N. Daldosso, R. Guider, D. Navarro-Urrios, A. Pitanti, R. Spano, and L. Pavesi, *Proc. IEEE* **97**, 1250 (2009).
- <sup>9</sup>Z. H. Lu, D. J. Lockwood, and J.-M. Baribeau, *Nature* **378**, 258 (1995).
- <sup>10</sup>G. F. Grom, D. J. Lockwood, J. P. McCaffrey, H. J. Labbe, P. M. Fauchet, B. White, Jr., J. Diener, D. Kovalev, F. Koch, and L. Tsybeskov, *Nature* **407**, 358 (2000).
- <sup>11</sup>M. Zacharias, J. Heitmann, R. Scholz, U. Kahler, M. Schmidt, and J. Bläsing, *Appl. Phys. Lett.* **80**, 661 (2002).
- <sup>12</sup>J.-M. Wagner, K. Seino, F. Bechstedt, A. Dymiaty, J. Mayer, R. Röfver, M. Först, B. Berghoff, B. Spangenberg, and H. Kurz, *J. Vac. Sci. Technol. A* **25**, 1500 (2007).
- <sup>13</sup>A. Anopchenko, A. Marconi, E. Moser, S. Prezioso, M. Wang, G. Pucker, P. Bellutti, and L. Pavesi, *J. Appl. Phys.* **106**, 033104 (2009).
- <sup>14</sup>A. Marconi, A. Anopchenko, M. Wang, G. Pucker, P. Bellutti, and L. Pavesi, *Appl. Phys. Lett.* **94**, 221110 (2009).
- <sup>15</sup>B. Gelloz and N. Koshida, in *Device Applications of Silicon Nanocrystals and Nanostructures*, edited by N. Koshida (Springer, New York, 2009), p. 25.
- <sup>16</sup>K. D. Hirschman, L. Tsybeskov, S. P. Duttagupta, and P. M. Fauchet, *Nature* **384**, 338 (1996).
- <sup>17</sup>M. Wang, A. Anopchenko, A. Marconi, E. Moser, S. Prezioso, L. Pavesi, G. Pucker, P. Bellutti, and L. Vanzetti, *Physica E* **41**, 912 (2009).
- <sup>18</sup>L. Vanzetti, G. Pucker, S. Milita, M. Barozzi, M. Ghulinyan, and M. Bersani, *Surf. Interface Anal.* **42**, 842 (2010).